Arabian Journal of Chemistry (2021) **14**, 103244

King Saud University

Arabian Journal of Chemistry

www.ksu.edu.sa
www.sciencedirect.com

ORIGINAL ARTICLE

Neighborhood M-polynomial of titanium compounds☆

Sourav Mondal [a], **Muhammad Imran** [b,*], **Nilanjan De** [c], **Anita Pal** [a]

[a] *Department of Mathematics, National Institute of Technology Durgapur, West Bengal 713209, India*
[b] *Department of Mathematical Sciences, United Arab Emirates University, Al Ain 15551, United Arab Emirates*
[c] *Department of Basic Sciences and Humanities (Mathematics), Calcutta Institute of Engineering and Management, Kolkata, India*

Received 6 April 2021; accepted 30 May 2021
Available online 05 June 2021

KEYWORDS

Graph;
Topological index;
Neighborhood M-polynomial;
Titania nanotube TiO_2;
Crystallographic structure TiF_2;

MSC (2010)
Primary: 05C35;
Secondary: 05C07; 05C40

Abstract The neighborhood M-polynomial is effective in recovering neighborhood degree sum based topological indices that predict different physical, chemical and biological characteristics of material under investigation. In this work, the neighborhood M-polynomial of Titania nanotube TiO_2 and the crystallographic structure of TiF_2 are obtained. From the neighborhood M-polynomial, some neighborhood degree sum based topological indices are recovered. Effect of oxygen vacancies on outcomes is discussed. A comparative study among the findings and some well-established degree-based indices is performed.

1. Introduction

Throughout this article, we consider connected graph without loops and parallel edges. Let $V(\Upsilon)$ and $E(\Upsilon)$ be node and edge sets of a graph Υ, accordingly. The degree (or valency) of a node $v \in V(\Upsilon)$, denoted by d_v, is the count of edges incident to v. Here δ_u denotes the degree sum of neighbors of u in Υ. By neighbors of a node, we mean the nodes adjacent to that node. Different properties and activities of a compound are closely related to its molecular graph and this issue is the main topic of interest in chemical graph theory. Quantitative structure–property/ quantitative structure–activity relationships (QSPR/QSAR) are mathematical models which relates the physico-chemical property/ biological activity of compounds to their chemical structures. It has been widely used as an important key field in drug discovery process for predicting physicochemical properties and biological activity of molecules. It expresses the characteristics of molecule through topological index without involving a wet lab. Topological index is a mapping from the collection of graphs to the set of real numbers that describe the topology of graph and are used in QSPR/QSAR analysis. It remains unchanged for isomorphic graphs. Topological indices can be computed by there usual definitions which is laborious while one intends to derive many indices of a certain category. To

* Corresponding author.
E-mail address: imrandhab@gmail.com (M. Imran).
☆ Peer review under responsibility of King Saud University.

Production and hosting by Elsevier

https://doi.org/10.1016/j.arabjc.2021.103244
1878-5352

overcome this approach, many algebraic polynomials (Hassani et al., 2013; Alamian et al., 2008; Farahani, 2013) have been introduced whose differentiation or integration or composition of both, obtained at a fixed point give topological indices. The M-polynomial (Deutsch and Klavzar, 2015; Kwun et al., 2017) is the most general polynomial to produce a large number of degree based topological indices. Rapid advances are created on a day-to-day basis to design fresh indices. Recently, some researchers put their attention on the neighborhood degree sum based indices (Hosamani, 2017; Mondal et al., 2021; Mondal et al., 2019; Mondal et al., 2021; Ghorbani and Hosseinzadeh, 2010; Ghorbani and Hosseinzadeh, 2013; Kulli, 2019; Kulli, 2019). To make the computation of these type of indices easier, present authors (Mondal et al., 2021; Verma et al., 2019) introduced the neighborhood M-polynomial (NM) whose function for neighborhood degree sum based indices is analogous to the function of the M-polynomial for degree based indices. Kwun et al. (2017) computed M-Polynomials and degree based topological indices of V-phenylenic nanotubes and nanotori. Present authors (Mondal et al., 2019) derived topological indices for praline graph of some graceful structures using M-polynomial. M-polynomial-based topological descriptors of chemical crystal structures and their applications were discussed in (Chu et al., 2020). M-polynomials and topological indices of linear chains of benzene, napthalene and anthracene were reported in (Li et al., 2020). Cancan et al. (2020) computed topological indices of silicate network via M-polynomial. M-polynomials and degree-based topological indices of the molecule copper (I) oxide were derived in (Chaudhry et al., 2021). Liu et al. (2019) obtained topological indices of nano-tubes via M-polynomial. Closed formulas of M-polynomial and topological descriptors of boron triangular nanotube were calculated in (Shin et al., 2020). M-polynomials of some nano-structures and zigzag edge coronoid fused by starphene were derived in (Raza et al., 2020; Afzal et al., 2020). Topological descriptors for the crystal structure of titanium difluoride TiF_2 were obtained in (Liu et al., 2018). Neighborhood degree sum based indices of molecular graphs were computed in (Mondal et al., 2021; Verma et al., 2019) using NM-polynomial. The M-polynomial and NM-polynomial of some anti-COVID-19 chemicals were evaluated in (Mondal et al., 2020).

One of the most rapidly and actively growing areas of modern science is the production of nanostructured materials of various geometric shapes, including nanowires, nanotubes, etc. The fascination with nanostructured materials stems from their physicochemical, structural, magnetic, and conductive properties, which differ significantly from bulk samples of similar composition. Kozlovskiy and Zdorovets (2020) presented the results of a study of the structural properties and phase composition of $Co/CoCo_2O_4$ nanowires obtained by electrochemical deposition into the pores of template matrices based on polyethylene terephthalate. Study of the effect of thermal annealing on the change in the structural properties and phase composition of metal Co nanostructures, as well as their use as a basis for lithium-ion batteries were reported in (Zdorovets and Kozlovskiy, 2019). Green synthesis for producing nanoparticles (NP) is a biological method which is safe, economical, eco-friendly and reduces the use of chemicals. Synthesis of Ag silver NP using an aqueous extract of Acorus Calamus rhizome was reported in (Sudhakar et al., 2015). To evaluate the antibacterial, antioxidant, and antitumor effects of obtained Ag silver NP, Nakkala et al. (2014) performed synthesis involving an aqueous extract of rhizome Acorus Calamus. Green synthesis of barium ferrite nanoparticles using rhizome extract of Acorus Calamus was reported in (Thakur et al., 2020). The synthesis of ceramic nanostructured materials with multifunctional characteristics is an important area of research related to the production and study of new materials. Zhumatayeva et al. (2020) reported the outcomes of a study of structural characteristics, as well as the possibility of using $Li_{0.15}Sr_{0.85}TiO_3$ ceramics as anode materials for lithium-ion batteries. Critical behavior of $La_{0.825}Sr_{0.175}MnO_{2.912}$ anion-deficient manganite in the magnetic phase transition region was analysed in (Trukhanov et al., 2007). Synthesis and structure of nanocrystalline manganite $La_{0.50}Ba_{0.50}MnO_3$ was described in (Trukhanov et al., 2008). Nano-structures based on iron-nickel compounds have found their application in biomedical applications, such as carriers for targeted drug delivery, bases for lithium-ion batteries, etc. Structures based on iron-cobalt compounds and their oxide forms are increasingly used as magnetic sensors. Kozlovskiy et al. (2020) reported the outcomes of the synthesis and subsequent phase transformations of FeCo nanowires depending on the annealing temperature. High chemical stability and corrosion resistance, in combination with functional magnetic properties of $BaFe_{12}O_{19}$ M-type hexaferrites or BaM opens up a wide range of possibilities for potential applications. Recently, the strong correlation of the heat treatment conditions (annealing), crystal structure parameters, microstructure and magnetic properties evolution in BaM nanohexaferrites is presented in (Trukhanov et al., 2021). Titanium is the ninth most plentiful metal in the Earth's crust. $TiO2$, the most common titanium chemical, has diverse uses from anti-corrosion, self-cleaning lubricants and paintings to solar panels and photocatalysts (Fujishima et al., 1999). The semi-conductive characteristics of TiO_2 nanotubes lead in a powerful ionic interaction between the support and an electrode, enhancing catalytic efficiency in redox rections. The TiO_2 nanotube is also used as electrode of dye-sensitized solar cells. Titanium difluoride is a water-insoluble form of titanium to use for oxygen-sensitive implementations like metal processing. Fluoride materials have a variety of applications in present technologies and research, from petroleum refining and coating to synthetic chemistry and pharmaceutical manufacturing. To design a nanotube and nanoparticle with the suggested characteristics, structurally delicate properties such as fracture strength and yield stress can be controlled. The topological index is a numeric measure of molecule that describes the topology of molecular graph under testing in several ways. That is why, researchers obtained different topological indices (Liu et al., 2018; Munir et al., 2016; De, 2016; Liu et al., 2016) for the aforesaid structures. In this work, our focus is on titanium based structures. We aim to obtain some neighborhood degree sum based indices of titania nanotube TiO_2 and crystallographic structure of TiF_2 via neighborhood M-polynomial approach.

The rest of the manuscript is constructed as follows. Section 2 contains some preliminaries required to obtain the main findings. Section 3 contains the methodology required to obtain the main results. Section 4 is divided into two subsections: first one deals with the computation of titania nanotube TiO_2 and the later contains the computation for crystallographic structure of TiF_2. The outcomes are compartively studied in Section 5. The work is concluded in Section 6.

2. Preliminaries

Topological indices based on degrees play a major role in the field of chemical graph theory among several classes of topological indices. Gutman and Trinajstić (1972) introduced the first degree-based molecular descriptor in 1972 which nowadays is known as Zagreb index. In 1975, Randić (1975) invented the branching index to characterize the molecular branching that was later renamed as connectivity index. Nowadays, most authors refer to it as to the Randić index. The degree based indices based on degree of end nodes of edges for a graph Υ are defined as follows:

$$I(\Upsilon) = \sum_{uv \in E(\Upsilon)} F(d_u, d_v),$$

where $F(d_u, d_v)$ is defined for different well-established descriptors in Table 1.

For more degree based indices, readers are referred to (Nagesh and Girish, 2020; De, 2018; De, 2018; Numan et al., 2021; De, 2019). The M-polynomial of a graph Υ is defined as,

$$M(\Upsilon; x, y) = \sum_{i \leqslant j} m_{(i,j)} x^i y^j. \tag{1}$$

Where $m_{(i,j)}$ is the total count of edges $uv \in E(\Upsilon)$ such that $\{d_u, d_v\} = \{i, j\}$. The neighborhood M-polynomial of a graph Υ is defined as,

$$NM(\Upsilon; x, y) = \sum_{i \leqslant j} \chi_{(i,j)} x^i y^j. \tag{2}$$

Where $\chi_{(i,j)}$ is the total count of edges $uv \in E(\Upsilon)$ such that $\{\delta_u, \delta_v\} = \{i, j\}$. We use $NM(\Upsilon)$ for $NM(\Upsilon; x, y)$ in this article. Now we set an example to describe aforesaid definitions. From Fig. 1, we have $d_a = 1, d_b = 2, d_c = 2, d_d = 1$, $\delta_a = 2, \delta_b = 3, \delta_c = 3, \delta_d = 2$. Thus, we have $m_{(1,2)} = 2, m_{(2,2)} = 1, \chi_{(2,3)} = 2, \chi_{(3,3)} = 1$. Therefore from Eqs. (1), (2), we have for n-butane, $M(G) = 2xy^2 + x^2y^2$, $NM(G) = 2x^2y^3 + x^3y^3$. Neighborhood degree sum based topological indices defined on edge collection of a graph Υ can be represented as

$$I(\Upsilon) = \sum_{uv \in E(\Upsilon)} f(\delta_u, \delta_v),$$

Table 1 Formulation of degree based topological indices.

$I(\Upsilon)$	$F(d_u, d_v)$	$I(\Upsilon)$	$F(d_u, d_v)$
First Zagreb index ($M_1(\Upsilon)$)(Gutman and Trinajstić, 1972)	$d_u + d_v$	Second Zagreb index ($M_2(\Upsilon)$) (Gutman and Trinajstić, 1972)	$d_u d_v$
Randić index ($R(\Upsilon)$)(Randić, 1975)	$\frac{1}{\sqrt{d_u d_v}}$	Forgotten topological index ($F(\Upsilon)$)(Furtula and Gutman, 2015)	$d_u^2 + d_v^2$
Inverse sum indeg index ($ISI(\Upsilon)$) (Vukicević and Gašperov, 2010)	$\frac{d_u d_v}{d_u + d_v}$	Redefined third Zagreb index ($ReZG_3(\Upsilon)$) (Ranjini et al., 2013)	$d_u d_v (d_u + d_v)$

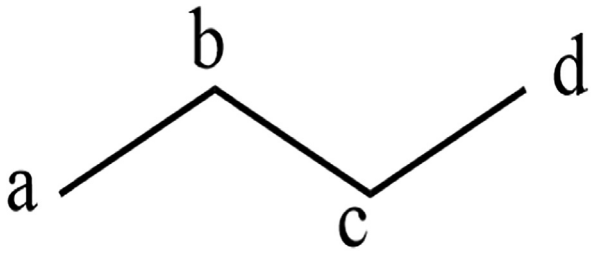

Fig. 1 Molecular graph of n-butane.

where $f(\delta_u, \delta_v)$ is the function of δ_u, δ_v used in Table 2 to formulate neighborhood degree sum based indices. The above formula can also be written as

$$I(\Upsilon) = \sum_{i \leqslant j} m_{(i,j)} f(i,j). \tag{3}$$

Formulations of neighborhood degree sum based indices and their relations with the NM-polynomial are shown in Table 2.

Here, $NM(\Upsilon)$ is a function of x, y and

$$D_x(NM(\Upsilon)) = x\frac{\partial(NM(\Upsilon))}{\partial x}, \; D_y(NM(\Upsilon)) = y\frac{\partial(NM(\Upsilon))}{\partial y},$$

Table 2 Formulation of topological indices using NM-polynomial for a graph Υ.

Topological Index	f(x,y)	Derivation from $NM(\Upsilon)$.
Third version of Zagreb index ($M_1'(\Upsilon)$) (Ghorbani and Hosseinzadeh, 2010)	$x + y$	$(D_x + D_y)(NM(\Upsilon))$ at $x = y = 1$
Neighborhood second Zagreb index ($M_2^*(\Upsilon)$) (Mondal et al., 2019)	xy	$(D_x D_y)(NM(\Upsilon))$ at $x = y = 1$
Neighborhood forgotten topological index ($F_N^*(\Upsilon)$) (Mondal et al., 2019)	$x^2 + y^2$	$(D_x^2 + D_y^2)(NM(\Upsilon))$ at $x = y = 1$
Neighborhood second modified Zagreb index (${}^{nm}M_2(\Upsilon)$) (Mondal et al., 2021)	$\frac{1}{xy}$	$(S_x S_y)(NM(\Upsilon))$ at $x = y = 1$
Neighborhood general Randić index($NR_\alpha(\Upsilon)$) (Mondal et al., 2021)	$(xy)^\alpha$	$(D_x^\alpha D_y^\alpha)(NM(\Upsilon))$ at $x = y = 1$
Third NDe index ($ND_3(\Upsilon)$) (Mondal et al., 2021)	$xy(x + y)$	$D_x D_y (D_x + D_y)(NM(\Upsilon))$ at $x = y = 1$
[1ex] Fifth NDe index ($ND_5(\Upsilon)$) (Mondal et al., 2021)	$\frac{x^2+y^2}{xy}$	$(D_x S_y + S_x D_y)(NM(\Upsilon))$ at $x = y = 1$
Neighborhood Harmonic index ($NH(\Upsilon)$) (Mondal et al., 2021)	$\frac{2}{x+y}$	$2S_x J(NM(\Upsilon))$ at $x = 1$
Neighborhood inverse sum index ($NI(\Upsilon)$) (Mondal et al., 2021)	$\frac{xy}{x+y}$	$S_x J D_x D_y(NM(\Upsilon))$ at $x = 1$
Sanskruti index ($S(\Upsilon)$) (Hosamani, 2017)	$\frac{xy}{(x+y-2)^3}$	$S_x^3 Q_{-2} J D_x^3 D_y^3 (NM(\Upsilon))$ at $x = 1$

$$S_x(NM(\Upsilon)) = \int_0^x \frac{(NM(\Upsilon))|_{x=z}}{z} dz,\ S_y(NM(\Upsilon)) = \int_0^y \frac{(NM(\Upsilon))|_{y=z}}{z} dz,$$

$$J(NM(\Upsilon)) = (NM(\Upsilon))|_{y=x},\ Q_\alpha(NM(\Upsilon)) = x^\alpha NM(\Upsilon).$$

For $\alpha = -\frac{1}{2}$ in NR_α, we have the fourth NDe index (Mondal et al., 2021) as follows:

$$ND_4(\Upsilon) = \sum_{uv \in E(\Upsilon)} \frac{1}{\sqrt{\delta_u \delta_v}}.$$

3. Methodology

The present work deals with some neighborhood degree sum based indices of two Titanium compounds: TiO_2 and TiF_2. First of all, the NM-polynomials of both the networks are computed and then using some calculus operators, different neighborhood degree sum based indices are recovered. We utilize combinatorial computation, graph theoretical tools and edge partition method to obtain the outcomes. The graphical representations of the results are shown using Maple 2015. A comparative study of the findings is performed via 3d line plotting in Matlab 2017.

4. Main results

In this section, we give our key analytical results and divide the section into two subsections.

4.1. *Computational aspects of Titania nanotubes $TiO_2[p, q]$*

In this section we consider the titania nanotube $TiO_2[p, q]$. The structure of the Titania nanotube $TiO_2[p, q]$ is depicted in Fig. 2. We compute the NM-polynomial of $TiO_2[p, q]$-nanotube in the following theorem.

Theorem 1. Let Υ be the $TiO_2[p, q]$-nanotube. Then we have,

$$NM(\Upsilon) = 2x^5y^7 + 2x^5y^{10} + 2qx^7y^9 + 2qx^7y^{13} + 4qx^8y^9 + 2qx^9y^{10} + 6px^9y^{11} + 3px^9y^{13} + 2q(2p+1)x^{10}y^{13} + 2q(p-1)x^{11}y^{13} + 2q(3p-2)x^{13}y^{13}.$$

Proof. The $TiO_2[p, q]$-nanotube has $12pq + 9p + 6q + 4$ number of edges. Its edge set can be partitioned as follows:

$$|E_{\{5,7\}}| = |\{uv \in E(\Upsilon) : \delta_u = 5, \delta_v = 7\}| = 2 = \chi_{(5,7)},$$

$$|E_{\{5,10\}}| = |\{uv \in E(\Upsilon) : \delta_u = 5, \delta_v = 10\}| = 2 = \chi_{(5,10)},$$

$$|E_{\{7,9\}}| = |\{uv \in E(\Upsilon) : \delta_u = 7, \delta_v = 9\}| = 2q = \chi_{(7,9)},$$

$$|E_{\{7,13\}}| = |\{uv \in E(\Upsilon) : \delta_u = 7, \delta_v = 13\}| = 2q = \chi_{(7,13)},$$

$$|E_{\{8,9\}}| = |\{uv \in E(\Upsilon) : \delta_u = 8, \delta_v = 9\}| = 4q = \chi_{(8,9)},$$

$$|E_{\{9,10\}}| = |\{uv \in E(\Upsilon) : \delta_u = 9, \delta_v = 10\}| = 2q = \chi_{(9,10)},$$

$$|E_{\{9,11\}}| = |\{uv \in E(\Upsilon) : \delta_u = 9, \delta_v = 11\}| = 6p = \chi_{(9,11)},$$

$$|E_{\{9,13\}}| = |\{uv \in E(\Upsilon) : \delta_u = 9, \delta_v = 13\}| = 3p = \chi_{(9,13)},$$

$$|E_{\{10,13\}}| = |\{uv \in E(\Upsilon) : \delta_u = 10, \delta_v = 13\}| = 2q(2p+1) = \chi_{(10,13)},$$

$$|E_{\{11,13\}}| = |\{uv \in E(\Upsilon) : \delta_u = 11, \delta_v = 13\}| = 2q(p-1) = \chi_{(11,13)},$$

$$|E_{\{13,13\}}| = |\{uv \in E(\Upsilon) : \delta_u = 13, \delta_v = 13\}| = 2q(3p-2) = \chi_{(13,13)}.$$

From the definition, the NM-polynomial of Υ is obtained as follows.

$$\begin{aligned} NM(\Upsilon) &= \sum_{i \le j} \chi_{(i,j)} x^i y^j \\ &= m_{(5,7)}x^5y^7 + m_{(5,10)}x^5y^{10} + m_{(7,9)}x^7y^9 + m_{(7,13)}x^7y^{13} \\ &+ m_{(8,9)}x^8y^9 + m_{(9,10)}x^9y^{10} + m_{(9,11)}x^9y^{11} + m_{(9,13)}x^9y^{13} \\ &+ m_{(10,13)}x^{10}y^{13} + m_{(11,13)}x^{11}y^{13} + m_{(13,13)}x^{13}y^{13}. \\ &= 2x^5y^7 + 2x^5y^{10} + 2qx^7y^9 + 2qx^7y^{13} + 4qx^8y^9 + 2qx^9y^{10} + 6px^9y^{11} \\ &+ 3px^9y^{13} + 2q(2p+1)x^{10}y^{13} + 2q(p-1)x^{11}y^{13} + 2q(3p-2)x^{13}y^{13}. \end{aligned}$$

This completes the proof. □

Now using this NM-polynomial, we calculate some neighborhood degree sum based indices of the $TiO_2[p, q]$-nanotube as follows.

Theorem 2. Let Υ be the $TiO_2[p, q]$-nanotube. Then we have,

1. $M_1'(\Upsilon) = 296pq + 186p + 72q + 54$,
2. $M_2^*(\Upsilon) = 1820pq + 945p + 74q + 170$,
3. $F_N^*(\Upsilon) = 3684pq + 1962p + 244q + 398$,

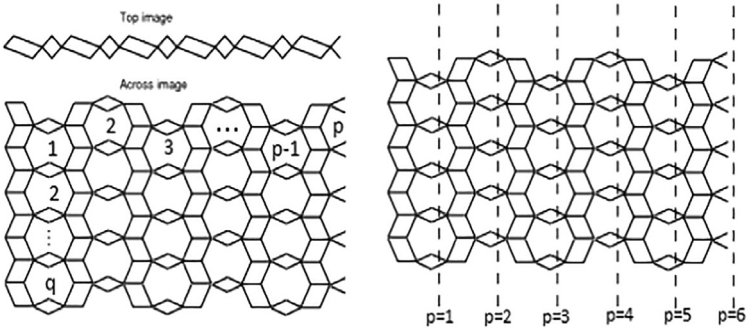

Fig. 2 The structure of $TiO_2[p, q]$-nanotubes, for $p = 6$ and $q = 4$.

4. ${}^{nm}M_2(\Upsilon) = 0.08pq + 0.086p + 0.109q + 0.097$,
5. $NR_\alpha(\Upsilon) = [4(130)^\alpha + 2(143)^\alpha + 6(13)^{2\alpha}]pq + [6(99)^\alpha + 3(117)^\alpha]p + [2(63)^\alpha + 2(91)^\alpha + 4(72)^\alpha + 2(90)^\alpha + 2(130)^\alpha - 2(143)^\alpha - 4(13)^{2\alpha}]q + 2[(35)^\alpha + (50)^\alpha]$,
6. $ND_3(\Upsilon) = 45188pq + 19602p - 4488q + 2340$,
7. $ND_5(\Upsilon) = 24.333pq + 18.653p + 13.078q + 9.228$,
8. $NH(\Upsilon) = 0.976pq + 0.873p + 0.831q + 0.6$,
9. $NI(\Upsilon) = 73.525pq + 45.654p + 16.778q + 12.5$,
10. $S(\Upsilon) = 3593.145pq + 1598.855p - 512.809q + 199.542$.

Proof. Let
$NM(\Upsilon) = f(x,y) = 2x^5y^7 + 2x^5y^{10} + 2qx^7y^9 + 2qx^7y^{13} + 4qx^8y^9 + 2qx^9y^{10} + 6px^9y^{11} + 3px^9y^{13} + 2q(2p+1)x^{10}y^{13} + 2q(p-1)x^{11}y^{13} + 2q(3p-2)x^{13}y^{13}$.

Then we have,

$$\begin{aligned}
(D_x + D_y)(f(x,y)) &= 24x^5y^7 + 30x^5y^{10} + 32qx^7y^9 + 40qx^7y^{13} + 68qx^8y^9 + 38qx^9y^{10} + 120px^9y^{11} + 66px^9y^{13} + 46q(2p+1)x^{10}y^{13} + 48q(p-1)x^{11}y^{13} + 52q(3p-2)x^{13}y^{13},\\
D_xD_y(f(x,y)) &= 70x^5y^7 + 100x^5y^{10} + 126qx^7y^9 + 182qx^7y^{13} + 288qx^8y^9 + 180qx^9y^{10} + 594px^9y^{11} + 351px^9y^{13} + 260q(2p+1)x^{10}y^{13} + 286q(p-1)x^{11}y^{13} + 338q(3p-2)x^{13}y^{13},\\
(D_x^2 + D_y^2)(f(x,y)) &= 148x^5y^7 + 250x^5y^{10} + 260qx^7y^9 + 436qx^7y^{13} + 580qx^8y^9 + 362qx^9y^{10} + 1212px^9y^{11} + 750px^9y^{13} + 538q(2p+1)x^{10}y^{13} + 580q(p-1)x^{11}y^{13} + 676q(3p-2)x^{13}y^{13},\\
S_xS_y(f(x,y)) &= \tfrac{2}{35}x^5y^7 + \tfrac{1}{25}x^5y^{10} + \tfrac{2}{63}qx^7y^9 + \tfrac{2}{91}qx^7y^{13} + \tfrac{1}{18}qx^8y^9 + \tfrac{1}{45}qx^9y^{10} + \tfrac{2}{33}px^9y^{11} + \tfrac{1}{39}px^9y^{13} + \tfrac{1}{65}q(2p+1)x^{10}y^{13} + \tfrac{2}{143}q(p-1)x^{11}y^{13} + \tfrac{2}{169}q(3p-2)x^{13}y^{13},\\
D_x^\alpha D_y^\alpha(f(x,y)) &= 2(35)^\alpha x^5y^7 + 2(50)^\alpha x^5y^{10} + 2q(63)^\alpha x^7y^9 + 2q(91)^\alpha x^7y^{13} + 4q(72)^\alpha x^8y^9 + 2q(90)^\alpha x^9y^{10} + 6p(99)^\alpha x^9y^{11} + 3p(117)^\alpha x^9y^{13} + 2q(2p+1)(130)^\alpha x^{10}y^{13} + 2q(p-1)(143)^\alpha x^{11}y^{13} + 2q(3p-2)(13)^{2\alpha}x^{13}y^{13},\\
D_xD_y(D_x + D_y)(f(x,y)) &= 840x^5y^7 + 1500x^5y^{10} + 2016qx^7y^9 + 3640qx^7y^{13} + 4896qx^8y^9 + 3420qx^9y^{10} + 11880px^9y^{11} + 7722px^9y^{13} + 5980q(2p+1)x^{10}y^{13} + 6864q(p-1)x^{11}y^{13} + 8788q(3p-2)x^{13}y^{13},\\
(D_xS_y + S_xD_y)(f(x,y)) &= \tfrac{148}{35}x^5y^7 + 5x^5y^{10} + \tfrac{260}{63}qx^7y^9 + \tfrac{436}{91}qx^7y^{13} + \tfrac{145}{18}qx^8y^9 + \tfrac{181}{45}qx^9y^{10} + \tfrac{404}{33}px^9y^{11} + \tfrac{250}{39}px^9y^{13} + \tfrac{269}{65}q(2p+1)x^{10}y^{13} + \tfrac{580}{143}q(p-1)x^{11}y^{13} + 4q(3p-2)x^{13}y^{13},\\
S_xJ(f(x,y)) &= \tfrac{1}{6}x^{12} + \tfrac{2}{15}x^{15} + \tfrac{1}{8}qx^{16} + \tfrac{1}{10}qx^{20} + \tfrac{4}{17}qx^{17} + \tfrac{2}{19}qx^{19} + \tfrac{3}{10}px^{20} + \tfrac{3}{22}px^{22} + \tfrac{2}{23}q(2p+1)x^{23} + \tfrac{1}{12}q(p-1)x^{24} + \tfrac{1}{13}q(3p-2)x^{26},\\
S_xJD_xD_y(f(x,y)) &= \tfrac{35}{6}x^{12} + \tfrac{20}{3}x^{15} + \tfrac{63}{8}qx^{16} + \tfrac{91}{10}qx^{20} + \tfrac{288}{17}qx^{17} + \tfrac{180}{19}qx^{19} + \tfrac{297}{10}px^{20} + \tfrac{351}{22}px^{22} + \tfrac{260}{23}q(2p+1)x^{23} + \tfrac{143}{12}q(p-1)x^{24} + 13q(3p-2)x^{26},\\
S_x^3Q_{-2}JD_x^3D_y^3(f(x,y)) &= 85.75x^{10} + 113.792x^{13} + 182.25qx^{14} + 258.426qx^{18} + 221.184qx^{15} + 296.764qx^{17} + 998.25px^{18} + 600.605px^{20} + 474.463q(2p+1)x^{21} + 549.25q(p-1)x^{22} + 698.323q(3p-2)x^{24}.
\end{aligned}$$

Rest of the proof can be done easily using Table 2. □

The topological indices for TiO_2 [p,q] are depicted in Fig. 3, Fig. 4 and Fig. 5.

Now putting $\alpha = -\frac{1}{2}$ in Theorem 2, we obtain the following corollary.

Corollary 1. *The fourth NDe index of TiO_2 [p,q] is given by*

$$ND_4(TiO_2[p,q]) = 0.9796pq + 0.8804p + 0.84439q + 0.621.$$

The vacancy defects, which are formed because of the absence of the atoms/ions from the lattice structure, are very common in all types of crystalline materials. Different properties of the titanium oxide-based nanomaterials are found to be explicitly dependent on the presence of various crystalline defects. Oxygen vacancies are the most frequent and foremost among them. Topological indices have two major subclasses: topostructural and topochemical. The former encode information strictly on molecular connectivity. The latter includes chemical features (atom and bond type) in addition to topological information. The present article deals with the topostructural indices. The argument of topostructural indices is always a molecular graph. By molecular graph of a chemical compound, we mean a simple connected graph whose vertices correspond to the atoms of the compound and edges correspond to chemical bonds (irrespective of bond type) between them. Thus, it is apparent that oxygen vacancies on TiO_2 crystal reduces the number of nodes and edges of the molecular graph. As a result, the indices derived from Theorem 2 and Corollary 1, will alter. For instance, M_1' moves down for imposing oxygen vacancy on TiO_2 crystal. Each of the indices considered in this work can model different physico-chemical properties with powerful accuracy (Hosamani, 2017; Mondal et al., 2019; Mondal et al., 2021; Ghorbani and Hosseinzadeh, 2013; Mondal et al., 2020). It is therefore clear that oxygen vacancies play vital role in governing and even drastically changing various physico-chemical properties of titanium dioxide nanostructures.

4.2. *Computational aspects of the crystallographic structure of TiF_2 [m, n, t].*

Here we consider the crystal structure of Titanium difluoride ($TiF_2[m,n,t]$). Its structure is shown in Fig. 6. The structure consists of $m \times n$ units in the plane and then stores them in t layers. We compute the NM-polynomial of the crystallographic structure of TiF_2 [m, n, t] as follows.

Theorem 3. Let Υ be the crystallographic structure TiF_2 [m, n, t]. Then we have,

$$\begin{aligned}
NM(\Upsilon) = {} & 8x^4y^{13} + 8(m+n+t-3)x^8y^{18} + 16x^{13}y^{16} + 8[2mn + 2mt + 2nt - 2m + 2n + 2t + 1]x^{16}y^{18} + 8[4mnt - 2(mn + mt + nt) + 1]x^{16}y^{24} + 8(m+n+t-2)x^{18}y^{32}.
\end{aligned}$$

Proof. The TiF_2 [m, n, t] structure has $32mnt$ number of edges. Its edge set has partitions as follows:

$$|E_{\{4,13\}}| = |\{uv \in E(\Upsilon) : \delta_u = 4, \delta_v = 13\}| = 8 = \chi_{(4,13)},$$

$$|E_{\{8,18\}}| = |\{uv \in E(\Upsilon) : \delta_u = 8, \delta_v = 18\}| = 8(m+n+t-3) = \chi_{(8,18)},$$

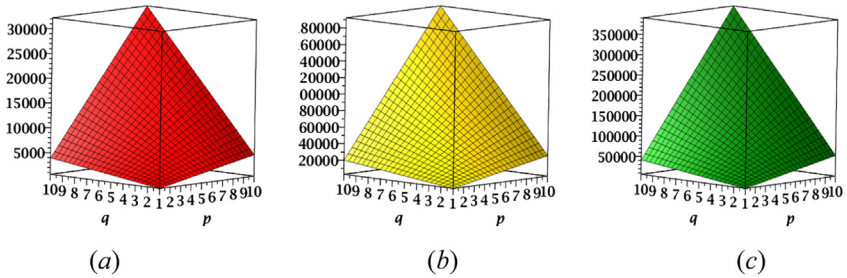

Fig. 3 (*a*) M_1', (b) M_2^*, and (c) F_N^* index of TiO_2 [p,q].

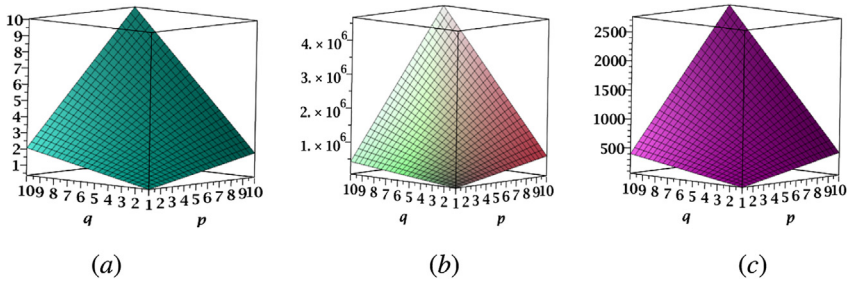

Fig. 4 (*a*) ${}^{mn}M_2$, (b) ND_3, and (c) ND_5 index of TiO_2 [p,q].

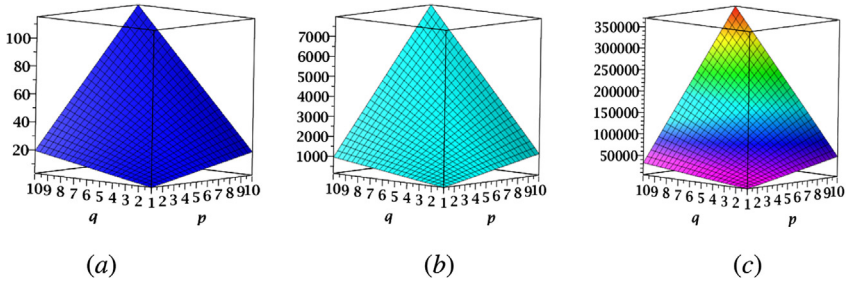

Fig. 5 (*a*) NH, (b) NI, and (c) S index of TiO_2 [p,q].

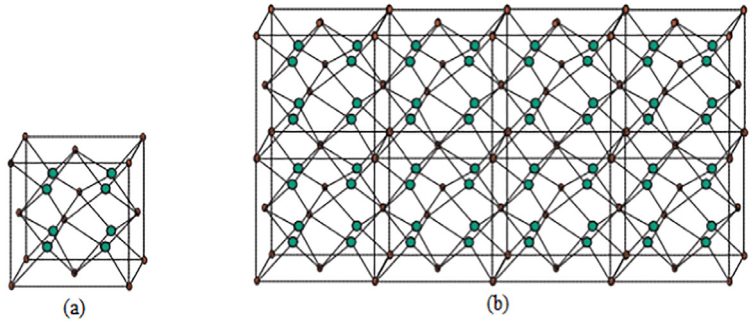

Fig. 6 (a) Unit cell of TiF_2 [m,n,t] (b) Crystallographic structure of TiF_2 [4,1,2].

$$| E_{\{13,16\}} | = | \{uv \in E(\Upsilon) : \delta_u = 13, \delta_v = 16\} | = 16 = \chi_{(13,16)},$$

$$| E_{\{16,24\}} | = | \{uv \in E(\Upsilon) : \delta_u = 16, \delta_v = 24\} | = 8[4mnt - 2mn - 2mt - 2nt + 1] = \chi_{(16,24)},$$

$$| E_{\{16,18\}} | = | \{uv \in E(\Upsilon) : \delta_u = 16, \delta_v = 18\} | = 8[2mn + 2mt + 2nt) - 2m + 2n + 2t + 1] = \chi_{(16,18)},$$

$$| E_{\{18,32\}} | = | \{uv \in E(\Upsilon) : \delta_u = 18, \delta_v = 32\} | = 8(m + n + t - 2) = \chi_{(18,32)}.$$

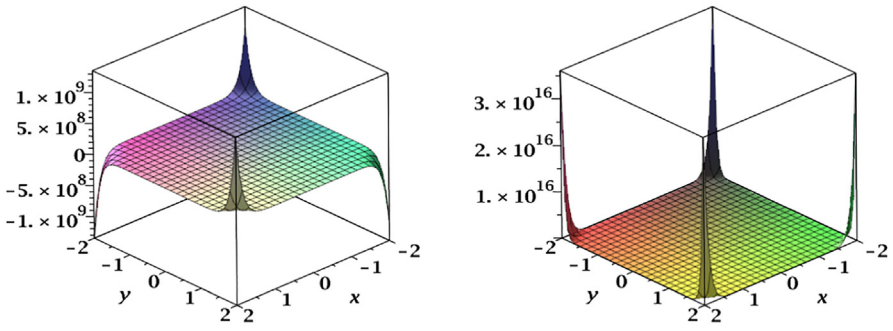

(*a*) (*b*)

Fig. 7 The *NM*-polynomal of (a) the $TiO_2[2,2]$-nanotube and (b) the crystallographic structure $TiF_2[2,2,2]$.

From the definition, the *NM*-polynomial of G can be obtained like previous. Hence the proof. □

The surface representation of NM-polynomials for both the networks is shown in Fig. 7. The range of x and y axes is taken arbitrarily from −2 to 2, as except for the vertical axis values, no changes would appear in the figures for the higher or lower range. It shows the changes of the *NM*-polynomial for varying its arguments. Now using this *NM*-polynomial, we calculate neighborhood degree sum based indices of the TiF_2 [m, n, t] structure in the following theorem.

Theorem 4. Let Υ be TiF_2 [m, n, t]. Then we have,

1. $M_1'(\Upsilon) = 1280mnt - 96mn - 96mt - 96nt + 64m + 64n + 64t - 232$,
2. $M_2^*(\Upsilon) = 12288mnt - 1536mn - 1536mt - 1536nt + 1152m + 1152n + 1152t - 3552$,
3. $F_N^*(\Upsilon) = 26624mnt - 4032mn - 4032mt - 4032nt + 4608m + 4608n + 4608t - 11304$,
4. ${}^{nm}M_2(\Upsilon) = 0.083mnt + 0.014mn + 0.014mt + 0.014nt + 0.014m + 0.014n + 0.014t + 0.085$,
5. $NR_\alpha(\Upsilon) = 8(52)^\alpha + 8(144)^\alpha(m+n+t-3) + 16(208)^\alpha + 8(288)^\alpha[2mn + 2mt + 2nt - 2m - 2n - 2t + 1] + 8(384)^\alpha[4mnt - 2mn - 2mt - 2nt + 1] + 8(576)^\alpha(m+n+t-2)$,
6. $ND_3(\Upsilon) = 491520mnt - 89088mn - 89088mt - 89088nt + 103720m + 103720n + 103720t - 245936$,
7. $ND_5(\Upsilon) = 69.333mnt - 2.444mn - 2.444mt - 2.444nt + 8.056m + 8.056n + 8.056t - 7.513$,
8. $NH(\Upsilon) = 1.6mnt + 0.141mn + 0.141mt + 0.141nt - 0.006m - 0.006n - 0.006t + 0.429$,
9. $NI(\Upsilon) = 307.2mnt - 18.07mn - 18.07mt - 18.07nt + 0.938m + 0.938n + 0.938t - 33.449$,
10. $S(\Upsilon) = 33021.2mnt - 4846.6mn - 4846.6mt - 4846.6nt + 3888m + 3888n + 3888t - 11096.333$.

Proof. Let $NM(\Upsilon) = f(x,y) = 8x^4y^{13} + 8(m+n+t-3)x^8y^{18} + > 16x^{13}y^{16} + 8[2mn + 2mt + 2nt - 2m - 2n - 2t + 1]x^{16}y^{18} + 8[4mnt - 2mn - 2mt - 2nt + 1]x^{16}y^{24} + 8(m+n+t-2)x^{18}y^{32}$.

Then we have,

$$
\begin{aligned}
(D_x + D_y)(f(x,y)) = {} & 136x^4y^{13} + 208(m+n+t-3)x^8y^{18} + > 464x^{13}y^{16} + 272[2mn + 2mt + 2nt - 2m - 2n - 2t + 1]x^{16}y^{18} + 320[4mnt - 2mn - 2mt - 2nt + 1]x^{16}y^{24} + 400(m+n+t-2)x^{18}y^{32},\\
D_xD_y(f(x,y)) = {} & 416x^4y^{13} + 1152(m+n+t-3)x^8y^{18} + 3328x^{13}y^{16} + 2304[2mn + 2mt + 2nt - 2m - 2n - 2t + 1]x^{16}y^{18} + 3072[4mnt - 2mn - 2mt - 2nt + 1]x^{16}y^{24} + 4608(m+n+t-2)x^{18}y^{32},\\
(D_x^2 + D_y^2)(f(x,y)) = {} & 1480x^4y^{13} + 3104(m+n+t-3)x^8y^{18} + 6800x^{13}y^{16} + 4640[2mn + 2mt + 2nt - 2m - 2n - 2t + 1]x^{16}y^{18} + 6656[4mnt - 2mn - 2mt - 2nt + 1]x^{16}y^{24} + 10784(m+n+t-2)x^{18}y^{32},\\
S_xS_y(f(x,y)) = {} & \tfrac{2}{13}x^4y^{13} + \tfrac{1}{18}(m+n+t-3)x^8y^{18} + \tfrac{1}{13}x^{13}y^{16} + \tfrac{1}{36}[2mn + 2mt + 2nt - 2m - 2n - 2t + 1]x^{16}y^{18} + \tfrac{1}{48}[4mnt - 2mn - 2mt - 2nt + 1]x^{16}y^{24} + \tfrac{1}{72}(m+n+t-2)x^{18}y^{32},\\
D_x^\alpha D_y^\alpha(f(x,y)) = {} & 8(52)^\alpha x^4y^{13} + 8(144)^\alpha(m+n+t-3)x^8y^{18} + 16(208)^\alpha x^{13}y^{16} + 8(288)^\alpha[2mn + 2mt + 2nt - 2m - 2n - 2t + 1]x^{16}y^{18} + 8(384)^\alpha[4mnt - 2mn - 2mt - 2nt + 1]x^{16}y^{24} + 8(576)^\alpha(m+n+t-2)x^{18}y^{32},\\
D_xD_y(D_x + D_y)(f(x,y)) = {} & 7072x^4y^{13} + 29952(m+n+t-3)x^8y^{18} + 96512x^{13}y^{16} + 78336[2mn + 2mt + 2nt - 2m - 2n - 2t + 1]x^{16}y^{18} + 122880[4mnt - 2mn - 2mt - 2nt + 1]x^{16}y^{24} + 230440(m+n+t-2)x^{18}y^{32},\\
(D_xS_y + S_xD_y)(f(x,y)) = {} & \tfrac{370}{13}x^4y^{13} + \tfrac{194}{9}(m+n+t-3)x^8y^{18} + \tfrac{425}{13}x^{13}y^{16} + \tfrac{145}{9}[2mn + 2mt + 2nt - 2m - 2n - 2t + 1]x^{16}y^{18} + \tfrac{52}{3}[4mnt - 2mn - 2mt - 2nt + 1]x^{16}y^{24} + \tfrac{337}{18}(m+n+t-2)x^{18}y^{32},\\
S_xJ(f(x,y)) = {} & \tfrac{8}{17}x^{17} + \tfrac{4}{13}(m+n+t-3)x^{26} + \tfrac{16}{29}x^{29} + \tfrac{4}{17}[2(mn+mt+nt) - 2(m+n+t) + 1]x^{34} + \tfrac{1}{5}[4mnt - 2mn - 2mt - 2nt + 1]x^{40} + \tfrac{4}{25}(m+n+t-2)x^{50},\\
S_xJD_xD_y(f(x,y)) = {} & \tfrac{416}{17}x^{17} + \tfrac{576}{13}(m+n+t-3)x^{26} + \tfrac{3328}{29}x^{29} + \tfrac{1152}{17}[2mn + 2mt + 2nt - 2m - 2n - 2t + 1]x^{34} + \tfrac{384}{5}[4mnt - 2mn - 2mt - 2nt + 1]x^{40} + \tfrac{2304}{25}(m+n+t-2)x^{50},\\
S_x^3Q_{-2}JD_x^3D_y^3(f(x,y)) = {} & 333.293x^{15} + 1728(m+n+t-3)x^{24} + 7315.074x^{27} + 5832[2mn + 2mt + 2nt - 2m - 2n - 2t + 1]x^{32} + 8255.3[4mnt - 2mn - 2mt - 2nt + 1]x^{38} + 13824(m+n+t-2)x^{48}.
\end{aligned}
$$

From Table 2, we can easily derive the required result. □

The topological indices for TiF_2 [m, n, 1] are depicted in Fig. 8, Fig. 9 and Fig. 10.

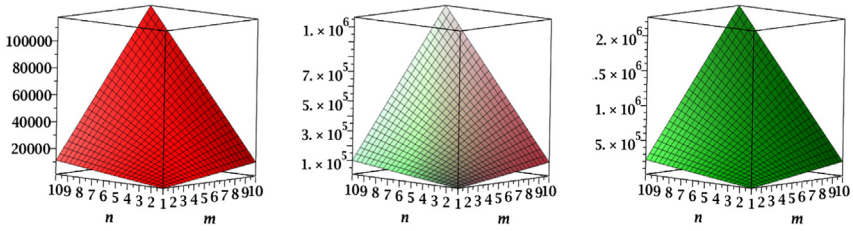

(a) (b) (c)

Fig. 8 (a) M_1', (b) M_2^*, and (c) F_N^* index of TiF_2 [m, n, 1].

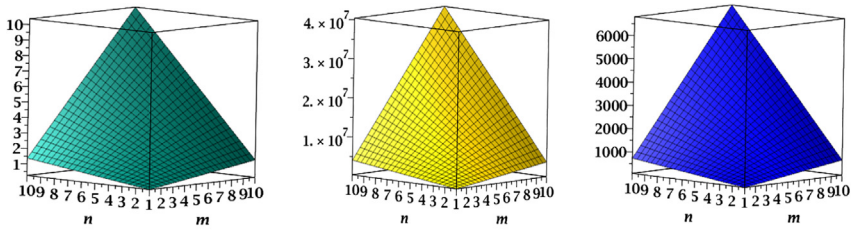

(a) (b) (c)

Fig. 9 (a) ${}^{mn}M_2$, (b) ND_3, and (c) ND_5 index of TiF_2 [m, n, 1].

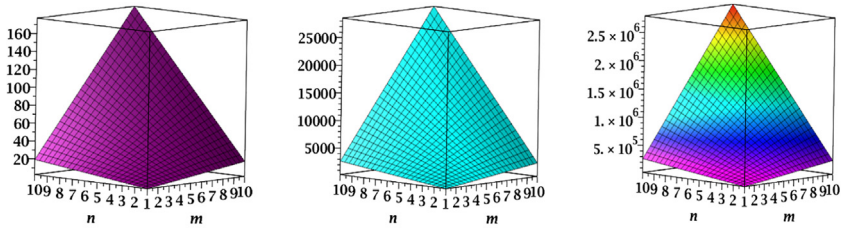

(a) (b) (c)

Fig. 10 (a) NH, (b) NI, and (c) S index of TiF_2 [m, n, 1].

Now putting $\alpha = -\frac{1}{2}$ in Theorem 2, we obtain the following corollary.

Corollary 2. The fourth NDe index of TiF_2 [m, n, t] is given by

$$ND_4(TiF_2[m,n,t]) = 0.9796pq + 0.8804p + 0.84439q + 0.621.$$

5. Comparative study

Firstly, we consider comparative study among different neighborhood degree sum based indices for the considered structures, later some well-known degree based indices reported in Table 1 are compared with present findings.

Different neighborhood degree sum based indices for TiO_2 [p,q] and TiF_2 [m, n, 1] are compared graphically in Fig. 11 and Fig. 12, respectively. From the Figs. 3,4,5,8,9,10,11,12,13,14, 15,16, following remarks can be drawn. In each compound under consideration, all indices respond diversely. In case of each index, the structures have the following order: T(TiO_2 [p,q])<T(TiF_2 [m, n, t]), T denotes the topological index. From the vertical axes of the figures, we can conclude that for both the structures, the neighborhood degree sum based indices have the following order: $ND_3 \geqslant F_N^* \geqslant M_2^* \geqslant M_1' \geqslant ND_5 \geqslant NI \geqslant ND_4 \geqslant NH \geqslant {}^{nm}M_2$. The ND_3 has the most dominating nature compared to other neighborhood degree sum based indices, whereas ${}^{m}NM_1$ grew slowly. The indices computed in this paper increase as well as graph parameters increase.

Many of the neighborhood degree sum based indices have similar formulations to degree based indices. Here we compare the behavior of the neighborhood degree sum based indices with their corresponding degree based indices for both the Titanium compounds through graphical representations. To plot degree based indices, explicit expressions of M_1, M_2, R, F, ISI, and $ReZG_3$ for TiO_2 [p,q] and TiF_2 [m,n,t] are collected from (Munir et al., 2016; Liu et al., 2018; De, 2016; Liu et al., 2016). From Figs. 13–16, one can say that neighborhood degree sum based descriptors show dominating nature over degree based descriptors except R and ND_4. From

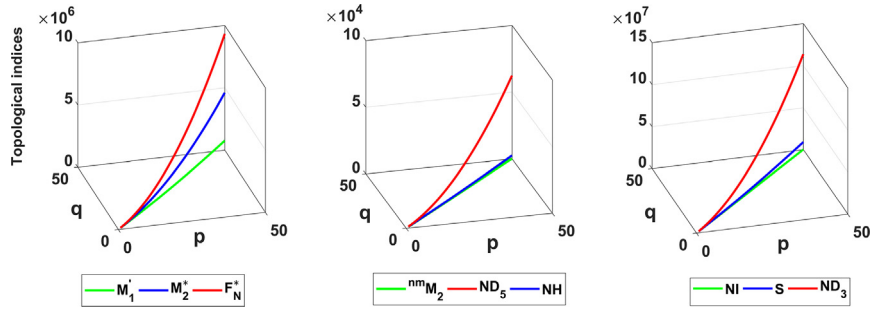

Fig. 11 Comparison of different topological indices for TiO_2 [p, q].

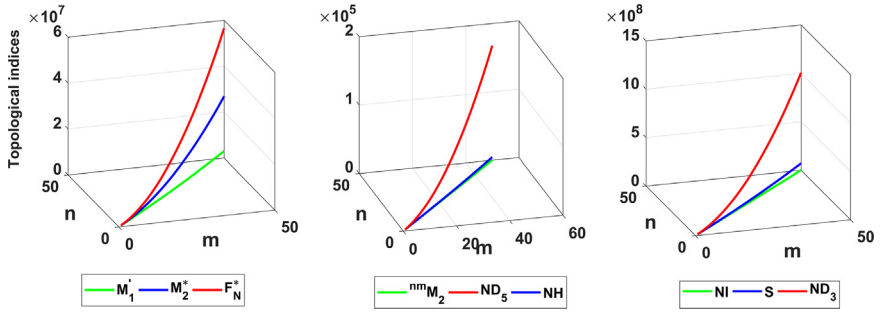

Fig. 12 Comparison of different topological indices for TiF_2 [m, n, 1].

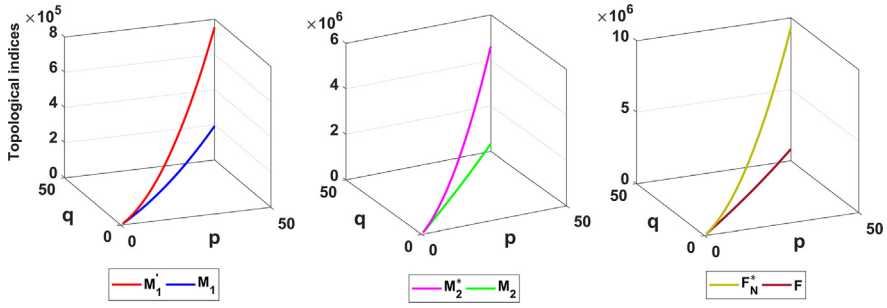

Fig. 13 Comparison of M_1', M_2^* and F_N^* indices with corresponding degree based indices for TiO_2 [p, q].

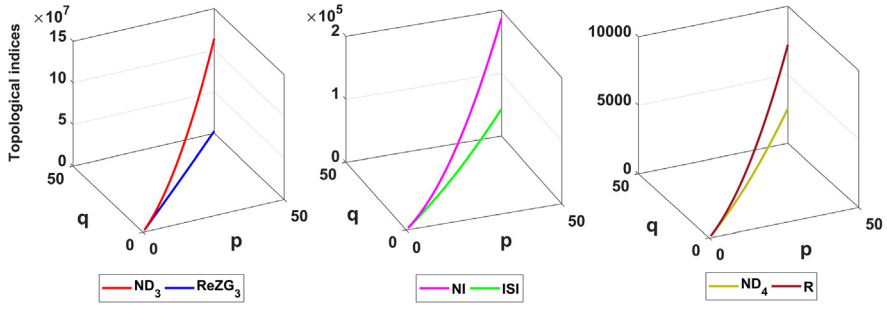

Fig. 14 Comparison of ND_3, NI and ND_4 indices with corresponding degree based indices for TiO_2 [p, q].

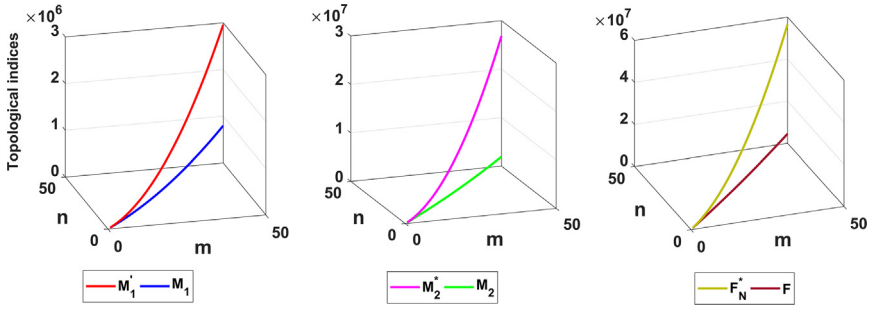

Fig. 15 Comparison of M_1', M_2^* and F_N^* indices with corresponding degree based indices for TiF_2 [m, n, 1].

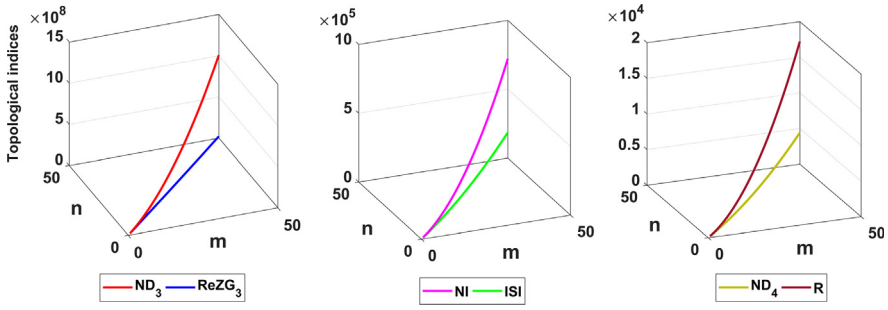

Fig. 16 Comparison of ND_3, NI and ND_4 indices with corresponding degree based indices for TiF_2 [m, n, 1].

Figs. 14, 16, it is clear to state that $R \geqslant ND_4$. There is therefore a sizable variation of the descriptors for the structures investigated.

6. Remarks and conclusions

In this article, we have studied the topological properties of the TiO_2 nanotube and the crystallographic structure of TiF_2. Firstly, the general form of neighborhood M-polynomial for the structures are obtained and then using that polynomials, some neighborhood degree sum based indices are recovered. To visualize the results, their graphical representations also have been made. Each of the indices considered in this work can model different physico-chemical properties with powerful accuracy. The correlation coefficients (r) of $M_1', M_2^*, F_N^*, {}^{nm}M_2, ND_3, NH$, and NI with entropy and acentric factor for octane isomers are $\geqslant 0.93$. Surprisingly, correlation coefficient of NI with acentric factor is 0.99. The correlation of ND_5 with different physico-chemical properties for alkanes is also notable ($r \geqslant 0.9$). Besides the structure–property/structure–activity modelling, a good descriptor should discriminate isomers. The isomer discrimination ability of neighborhood degree sum based indices is remarkable in comparison with degree based indices. Thus the considered indices are useful to describe the structural features of molecular graph. The computation of such indices of aforesaid useful structures is therefore worth-while and the findings can be helpful to understand the topology of the structures.

Declaration

Ethics approval and consent to participate

Not applicable.

Consent for publication

Not applicable.

Availability of data and material

Not applicable.

Funding

This work was supported by the United Arab Emirates University [Award Number: G00003271].

Authors' contributions

SM- Conceptualization, Writing- Original draft preparation, Software; ND- Investigation, Writing- Reviewing and Editing; MI-Writing-Original draft preparation; AP- Supervision, Validation.

Declaration of Competing Interest

The authors declare that they have no known competing financial interests or personal relationships that could have appeared to influence the work reported in this paper.

Acknowledgments

The first author is obliged to the Department of Science and Technology (DST), Government of India for the Inspire Fellowship [IF170148].

References

Afzal, F., Hussain, S., Afzal, D., Hameed, S., 2020. M-polynomial and topological indices of zigzag edge coronoid fused by starphene. Open Chemistry 18 (1), 1362–1369.

Alamian, V., Bahrami, A., Edalatzadeh, B., 2008. PI Polynomial of V-Phenylenic nanotubes and nanotori. Int. J. Mole. Sci. 9 (3), 229–234.

Cancan, M., Afzal, D., Hussain, S., Maqbool, A., Farkhanda, A., 2020. Some new topological indices of silicate network via M-polynomial. J. Discret. Math. Sci. Cryptogr. 23 (6), 1157–1171.

Chaudhry, F., Shoukat, I., Afzal, D., Park, C., Cancan, M., Farahani, M.R., 2021. M-Polynomials and Degree-Based Topological Indices of the Molecule Copper(I) Oxide. J. Chem. 2021, 6679819.

Chu, Y.M., Imran, M., Baig, A.Q., Akhter, S., Siddiqui, M.K., 2020. On M-polynomial-based topological descriptors of chemical crystal structures and their applications. Eur. Phys. J. Plus 135, 874.

De, N., 2016. On Molecular Topological Properties of TiO2 Nanotubes. Journal of Nanoscience. 2016, 1–5. https://doi.org/10.1155/2016/1028031.

De, N., 2018. Hyper Zagreb index of bridge and chain graphs. Open J. Math. Sci. 2 (1), 1–17.

De, N., 2018. Computing reformulated first Zagreb index of some chemical graphs as an application of generalized hierarchical product of graphs. Open J. Math. Sci. 2 (1), 338–350.

De, N., 2019. General Zagreb index of some cactus chains. Open Journal of Discrete Applied Mathematics 2 (1), 24–31.

Deutsch, E., Klavzar, S., 2015. M-Polynomial, and degree-based topological indices Iran. J. Math. Chem. 6 (2), 93–102.

Farahani, M.R., 2013. Computing theta polynomial, and theta index of V-phenylenic planar, nanotubes and nanotoris. Int. J. Theoretical Chem. 1 (1), 1–9.

Fujishima, A., Hashimoto, K., Watanabe, T., 1999. TiO2 Photocatalysis: Fundamentals and Applications. BKC, Tokyo.

Furtula, B., Gutman, I., 2015. A Forgotten topological index. J. Math. Chem. 53, 1184–1190.

Ghorbani, M., Hosseinzadeh, M.A., 2010. A note of Zagreb indices of nanostar dendrimers. Optoelectron. Adv. Mater. - Rapid Comm. 4 (11), 1877–1880.

Ghorbani, M., Hosseinzadeh, M.A., 2013. The third version of Zagreb index. Discrete Math. Algorithms Appl. 5 (4), 1350039.

Gutman, I., Trinajstić, N., 1972. Graph theory and molecular orbitals. Total <texmath type="inline">phi</texmath>-electron energy of alternant hydrocarbons. Chem. Phys. Lett. 17, 535–538.

Hassani, F., Iranmanesh, A., Mirzaie, S., 2013. Schultz and Modified Schultz Polynomials of C100 Fullerene. MATCH Commun. Math. Comput. Chem. 69, 87–92.

Hosamani, S.M., 2017. Computing Sanskruti index of certain nanostructures. J. Appl. Math. Comput. 54, 425–433.

Kozlovskiy, A.L., Zdorovets, M.V., 2020. The study of the structural characteristics and catalytic activity of Co/CoCo2O4 nanowires. Compos. B: Eng. 191, 107968.

Kozlovskiy, A.L., Kenzhina, I.E., Zdorovets, M.V., 2020. FeCo-Fe2CoO4/Co3O4 nanocomposites: Phase transformations as a result of thermal annealing and practical application in catalysis. Ceram. Int. 46, 10262–10269.

Kulli, V.R., 2019. Neighborhood Indices of Nanostructures. International Journal of Current Research in Science and Technology 5 (3), 1–14.

Kulli, V.R., 2019. Multiplicative Neighborhood Indices. Annuls of Pure and Applied Mathematics. 19 (2), 175–181.

Kwun, Y.C., Munir, M., Nazeer, W., Rafque, S., Kang, S.M., 2017. M-Polynomials and topological indices of V-Phenylenic Nanotubes and Nanotori. Sci. Rep. 7, 8756.

Li, C.P., Zhonglin, C., Munir, M., Yasmin, K., Liu, J.B., 2020. M-polynomials and topological indices of linear chains of benzene, napthalene and anthracene. Math. Biosci. Eng. 17 (3), 2384–2398.

Liu, J.B., Gao, W., Siddiqui, M.K., Farahani, M.R., 2016. Computing three topological indices for Titania nanotubes TiO_2. AKCE International Journal of Graphs and Combinatorics 13 (3), 255–260.

Liu, J.B., Siddiqui, M.K., Zahid, M.A., Naeem, M., Baig, A.Q., 2018. Topological Properties of Crystallographic Structure of Molecules. Symmetry 10 (7), 265.

Liu, J.B., Younas, M., Habib, M., Yousaf, M., Nazeer, W., 2019. M-polynomials and degree-based topological indices of $VC_5C_7[p, q]$ and $VC_5C_7[p, q]$ Nanotubes. IEEE Access 7, 41125–41132.

Mondal, S., De, N., Pal, A., 2019. The M-Polynomial of Line graph of Subdivision graphs. Commun. Fac. Sci. Univ. Ank. Ser. A1 Math. Stat. 68 (2), 2104–2116.

Mondal, S., De, N., Pal, A., 2019. On some new neighbourhood degree based indices. Acta Chemica Iasi 27 (1), 31–46.

Mondal, S., De, N., Pal, A., 2020. Topological Indices of Some Chemical Structures Applied for the Treatment of COVID-19 Patients. Polycycl Aromat Compd. https://doi.org/10.1080/10406638.2020.1770306.

Mondal, S., De, N., Pal, A., 2020. Molecular descriptors of neural networks with chemical significance. Rev. Roum. Chim. 65, 1039–1052.

Mondal, S., Siddiqui, M.K., De, N., Pal, A., 2021. Neighborhood M-polynomial of crystallographic structures. Biointerface Res. Appl. Chem. 11 (2), 9372–9381.

Mondal, S., De, N., Pal, A., 2021. On Neighbourhood Zagreb index of product graphs. J. Mol. Struct. 1223, 129210.

Mondal, S., Dey, A., De, N., Pal, A., 2021. QSPR analysis of some novel neighborhood degree based topological descriptors. Complex Intell. Syst. 7, 977–996.

Munir, M., Nazeer, W., Nizami, A.R., Rafique, S., Kang, S.M., 2016. M-Polynomials and Topological Indices of Titania Nanotubes. Symmetry 8 (11), 117.

Nagesh, H.M., Girish, V.R., 2020. On the entire Zagreb indices of the line graph and line cut-vertex graph of the subdivision graph. Open J. Math. Sci. 4 (1), 470–475.

Nakkala, J.R., Mata, R., Gupta, A.K., Sadras, S.R., 2014. Biological activities of green silver nanoparticles synthesized with acorous calamus rhizome extract. Eur. J. Med. Chem. 85, 784–794.

Numan, M., Butt, S.I., Taimur, A., 2021. Super cyclic antimagic covering for some families of graphs. Open J. Math. Sci. 5 (1), 27–33.

Randić, M., 1975. Characterization of molecular branching. J. Am. Chem. Soc. 97, 6609–6615.

Ranjini, P.S., Lokesha, V., Usha, A., 2013. Relation between phenyleneand hexagonal squeeze using harmonic index. Int. J. Graph Theory 1, 116–121.

Raza, Z., Essa, K., Sukaiti, M., 2020. M-Polynomial and Degree Based Topological Indices of Some Nanostructures. Symmetry. 12 (5), 831.

Shin, D.Y., Hussain, S., Afzal, F., Park, C., Afzal, D., Farahani, M. R., 2020. Closed Formulas for Some New Degree Based Topological Descriptors Using M-polynomial and Boron Triangular Nanotube. Front Chem. 8, 613873.

Sudhakar, C., Selvam, K., Govarthanan, M., Senthilkumar, B., Sengottaiyan, A., Stalin, M., Selvankumar, T., 2015. Acorus calamus rhizome extract mediated biosynthesis of silver nanoparticles and their bactericidal activity against human pathogens. J. Genetic Eng. Biotech. 13, 93–99.

Thakur, A., Sharma, N., Bhatti, M., Sharma, M., Trukhanov, A.V., Trukhanov, S.V., Panina, L.V., Astapovich, K.A., Thakur, P., 2020. Synthesis of barium ferrite nanoparticles using rhizome extract of Acorus Calamus: Characterization and its efficacy against different plant phytopathogenic fungi. Nano-Struct. Nano-Objects. 24, 100599.

Trukhanov, S.V., Trukhanov, A.V., Vasil'ev, A.N., Maignan, A., Szymczak, H., 2007. Critical behavior of $La_{0.825}Sr_{0.175}MnO_{2.912}$ anion-deficient manganite in the magnetic phase transition region. JETP Lett. 85, 507–512.

Trukhanov, S.V., Fedotova, V.V., Trukhanov, A.V., Stepin, S.G., Szymczak, H., 2008. Synthesis and structure of nanocrystalline $La_{0.50}Ba_{0.50}MnO_3$. Crystallogr. Rep. 53, 1177–1180.

Trukhanov, A.V., Darwish, K.A., Salem, M.M., Hemeda, O.M., Abdel, A.M.I., Darwish, M.A., Kaniukov, E.Y., Podgornaya, S.V., Turchenko, V.A., Tishkevich, D.I., Zubar, T.I., Astapovich, K.A., Kostishyn, V.G., Trukhanov, S.V., 2021. Impact of the heat treatment conditions on crystal structre, morphology and magnetic properties evolution in BaM nanohexaferrites. J. Alloys Compd. 866, 158961.

Verma, A., Mondal, S., De, N., Pal, A., 2019. Topological Properties of Bismuth tri-iodide Using Neighborhood M-Polynomial. International Journal of Mathematics Trends and Technology 65 (10), 83–90.

Vukicević, D., Gašperov, M., 2010. Bond additive modeling 1. Adriatic indices. Croat. Chem. Acta. 83, 243–260.

Zdorovets, M.V., Kozlovskiy, A.L., 2019. Investigation of phase transformations and corrosion resistance in Co/CoCo2O4 nanowires and their potential use as a basis for lithium-ion batteries. Sci. Rep. 9, 16646.

Zhumatayeva, I.Z., Kenzhina, I.E., Kozlovskiy, A.L., Zdorovets, M. V., 2020. The study of the prospects for the use of Li0.15Sr0.85-TiO3 ceramics. J. Mater. Sci.: Mater. Electron. 31, 6764–6772.